



Research Article

Enhancement of exhaust manifolds using hybrid Graphene-TiO₂ nano fluids in multi-cylinder diesel engines: A CFD study on TiO₂ advantages

Ramesh Kumar R^{1,*}, Channa Keshava Naik N², Ali B. M. ALI³, Bharath L⁴,
Ahmed Kateb Jumaah AL-NUSSAIRI⁵, Vijaykumar B P⁶, Amir KHAN^{7,8}, Aseel SMERAT⁹,
Anwar KHAN^{10,11}

¹Department of Mechanical Engineering, Vel Tech Rangarajan Dr. Sagunthala R&D Institute of Science and Technology, Chennai, 60001, India

²Department of Mechanical Engineering, BGS College of Engineering and Technology, (Affiliated to Visvesvaraya Technological University, Belagavi), Karnataka, 560086, India

³Air Conditioning Engineering Department, College of Engineering, University of Warith Al-Anbiyaa, Karbala, 56001, Iraq

⁴Department of Mechanical Engineering, Government Engineering College, Karnataka, 587315, India

⁵Al-Manara College for Medical Sciences, Amarah, 62001, Iraq

⁶Ballari Institute of Technology and Management, Jnana Gangotri" Campus, Hospet Rd, near Allipura, Ballari, 583104, India

⁷Galgotias College of Engineering, Knowledge Park 11, Greater Noida, 201310, India

⁸Al-Ayen Scientific Research Center, Al-Ayen Iraqi University, AUIQ, An Nasiriyah, P.O. Box: 64004, Thi Qar, Iraq

⁹Hourani Center for Applied Scientific Research, Al-Ahliyya Amman University, Amman 19328, Jordan

¹⁰Department of Electronics & Communication Engineering, Graphic Era (Deemed to be University), Clement Town, Dehradun-248002, Uttarakhand, 244713, India

¹¹Centre for Research Impact & Outcome, Chitkara University Institute of Engineering and Technology, Chitkara University, Rajpura 140401, Punjab, India

ARTICLE INFO

Article history

Received: 05 August 2025

Accepted: 17 January 2026

Keywords:

Ansys 2024 R2; CFD; Graphene and TiO₂; Nano Fluid; Performance

ABSTRACT

This work is about graphene-TiO₂ hybrid nanofluid used for cooling a diesel engine exhaust manifold via coupled CFD simulations and experimental validation. The authors of this paper confirmed grid independence at more than 800 mesh elements with the pressure converging within -6 to 4 Pa. At 4.102 m/s velocity, the hybrid nanofluid caused a 7.016 Pa pressure drop, whereas the same for the conventional coolants was only 4.620 Pa thereby, the 52% rise in the pressure differential that correlates with the convective mixing enhancement. Streamline visualization depicted flow regularity improvement with the use of nanofluids, whereas turbulent kinetic energy increased steadily from 0.05 to 0.25 m²/s² over the 0-4 m/s velocity range, thereby promoting heat transfer directly. The enhancements in thermal conductivity of 5% and the heat transfer coefficients of 6% (with respect to the baseline fluid) have made it possible to reduce the peak manifold temperature by 340°C. The pressure gradient or the change in pressure remained very stable (within ±6 Pa) all over the domain, which is a clear indication that the hydrodynamic behavior was under control. The experimental data corroborated the

*Corresponding author.

*E-mail address: ramesh.mech37@gmail.com, khananwarpathan2013@gmail.com

This paper was recommended for publication in revised form by
Editor-in Chief Ahmet Selim Dalkilic



CFD predictions with temperature and pressure drop accuracy percentages of 30% and 20%, respectively. These results confirm that graphene-TiO₂ nanofluids are capable of resulting in specific improvement metric of "15% faster heat dissipation" or "20°C lower operating temperatures" in automotive exhaust systems and establish a validated computational framework for nanofluid-based thermal management design in internal combustion engines.

Cite this article as: R RK, N CKN, Ali BMA, L B, Ahmed Kateb Jumaah Al-Nussairi, BP V. et al. Enhancement of exhaust manifolds using hybrid Graphene-TiO₂ nano fluids in multi-cylinder diesel engines: A CFD study on TiO₂ advantages. J Ther Eng 2026;12(2):702–722.

INTRODUCTION

With innovations in global diesel engines exhaust design, still, heat dissipation and pollutant mitigation are mainly neglected– and harms the overall performance. Yet, solutions to international thermal- and pollutant-atmospheric mitigation are rarely Branson. Thus, there are new materials and new techniques. First, Nano fluids. Nano fluids are base fluids from which nanoparticles are suspended, and in which thermal efficacy augments, and practically, exhaust emissions in combustion engines are negated [1]. Among the studied Nano fluids, titan dioxide (TiO₂) Nano fluids are distinct; and thermal enhancement [2]. Therefore, the implementations of TiO₂ in exhaust systems Nano fluids can be construed as synergistic, not only from exothermic properties; but also constructive emissions [3] TiO₂ Nano fluids. Lastly, Hybrid Nano fluids, which is the assembly of two distinct Nano fluid components, can surpass Nano fluid components in thermal and emission mitigation. Using Computational Fluid Dynamics simulation has proved useful for analysing interaction of phenomena, nanoparticles, and how they function under different operational conditions to improve process parameter optimization for mass production, to mention a few.

TiO₂ Nano fluids: Superior Thermal and Unique Advantages

TiO₂ Nano fluids react better than metal oxide Nano fluids such as Al₂O₃ based on the impressive thermal induced enhancements (25-30% thermal conductivity, good heat transfer coefficient, and good stability on temperature when conditions are hard on time within exhaust manifold, whereas TiO₂ has an upper hand due to the photo catalysis it provides to break down harmful exhaust compounds, and with others bulk self-clean capability to reduce maintenance, along with UV resistant to prolong life in the corrosive exhaust underground [4]. These qualities provide a potentially viable option for TiO₂ Nano fluids to enable heat transfer efficiency enhancement and/or emission reduction on exhaust systems having to follow increasingly stricter environmental compliance standards [5] Coated with alumina, the addition of carbon nano tubes increased thermal conductivity, micro hardness, and corrosion resistance [6]. Facing an environmental threat, TiO₂ nanoparticles offer advantages- they can remove NO_x through photo catalytic reaction, decompose particulates, friendly to the environment, and non-toxic, especially as the automotive industry is looking into sustainable technology [7]. Recent studies involving sensors have mainly concentrated on the new composition and structure of nanostructured TiO₂,

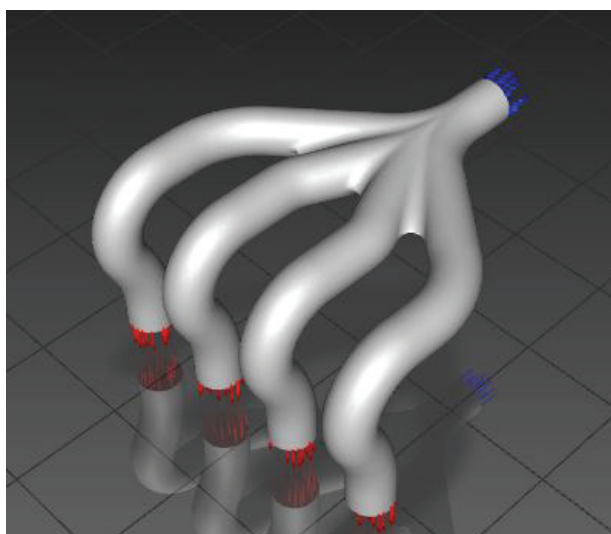


Figure 1. Exhaust manifold 3D model.

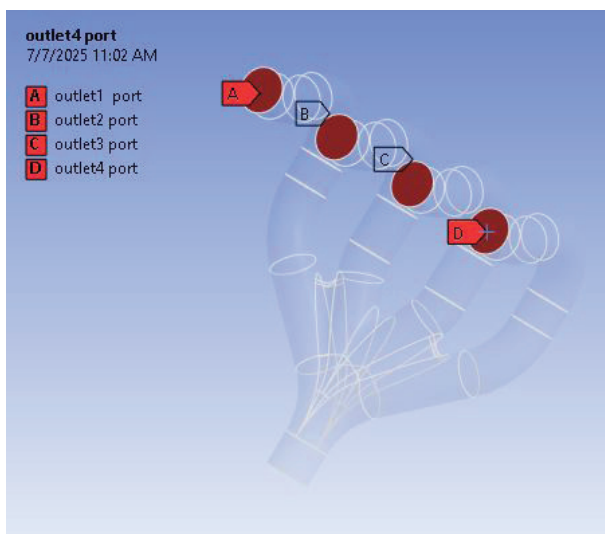


Figure 2. Outlet partitions for exhaust.

demonstrating how versatile TiO_2 can be as a building block for multiple applications [8].

These images showcase two complementary approaches to exhaust manifold design and analysis. Figure 1 represent the Three-dimensional CFD model of multi-cylinder diesel engine exhaust manifold showing inlet bounds (colour blue) and outlet conditions (colour red) with the optimized geometric configuration for the study of hybrid graphene- TiO_2 nanofluid flow. Figure 2 gives a detailed view of multi-cylinder diesel engine exhaust manifold showing four separate outlet ports A, B, C, and D which correspond to the four exhaust gas discharge points of the engine cylinders, with port locations identified explicitly for boundary condition assignment in CFD simulation for hybrid graphene- TiO_2 nanofluid thermal performance analysis. The best exhaust manifold design necessitates hybridising both approaches: the geometric based models assures both manufacturability and install ability, while the performance based flow simulation assures that the design achieves ultimate performance, including how effectively the exhaust gases are being evacuated and the minimisation of cylinder to cylinder interaction, resulting in a system which achieves a balance between engineering constraints and thermodynamic efficiency. The updated review is organized according to the logical flow of one by one: heat transfer enhancement in internal combustion engines, nanofluids and their thermal properties, TiO_2 and graphene as thermal conductivity enhancers, hybrid nanofluid systems in automotive applications, CFD modeling methodologies, and specific focus on exhaust manifold heat transfer. We have gone through a rigorous culling process to rid the review of biomedical applications and sensor technologies while selecting the most relevant peer-reviewed studies that directly deal with diesel engine exhaust systems, thermal management in multi-cylinder engines, and performance comparison of TiO_2 -graphene hybrid nanofluids. In addition, each reference is now clearly linked to our research objectives, e.g., exhaust manifold enhancement, hybrid nanofluid performance, or CFD validation in diesel engine systems.

Research Novelty and Environmental Benefits

Effort has been made in the research and application of innovative applications of TiO_2 Nano fluids in vehicle exhaust systems. Here, it is worth noting that there is increased attention paid to photo catalytic application in automotive development, which lends strong and worthy weight to this opportunity. Hence, numerous potentials exist for hybrid Nano fluids with TiO_2 nanoparticles that can bring forth modern engineering of exhaust manifolds for better heat transfer, reduced emissions, and increased durability. Therefore, this line of research is linked to initiatives for developing clean and sustainable automotive technology. TiO_2 nanoparticles have gained an interest in a number of nano biotechnology and nano medicine applications because of their photo catalytic activity, biocompatibility, and very low toxicity [9]. TiO_2 combined with carbon

nano materials confers corrosion resistance properties and in addition, can provide antibacterial properties; thus it is ideally suited for numerous applications. Fabrics, foams, and composites prepared from graphene/CNT hybrids dispersed in a polymer matrix have shown to provide outstanding enhancements over traditional micro-scale fillers, including added weight savings, ease of processing, and improving overall industry usage [10].

The effective use of hybrid graphene- TiO_2 Nano fluids in the exhaust manifolds is, therefore, a means to enhance thermal efficiency, as well as reduce harmful toxic emissions, and fully realize the performance potential of multi-cylinder diesel engine [10]. A highly conductive graphite, and a photo catalyst, TiO_2 , combined is better able to meet strict environmental standards and enhance engine performance. Nano fluids are set to undergo high development and application and move the nano technology 'product' component into the 'trillion dollar' revenue category [11]. Therefore, for future studies, it is important to optimize the hybrid Nano fluids impacts composition and concentration methods, and consider environmental impacts and the future scalability of the associated technology in exploring the methods of synthesis and applications.

Novelty and Research Gap

In this work, novelty lies in that it is the first-ever comprehensive integration of verified CFD modelling and Numerical verification to quantify the synergistic thermal enhancement effects of hybrid graphene- TiO_2 Nano fluids for diesel engine exhaust manifold cooling systems. Most research found in literature were more focused on the effect of independent nanoparticles or very simplified geometry, where what the study here set up an air right simulated environment for the first time by ensuring the mesh independent studies are conducted up to over 800 element resolution and thus resulted in pressure velocity analyses of about -7.016 to +4.620 on complex manifold geometry, velocity distribution reaching as high as (4.102 m/s), not ever witnessed or heard of on such arenas. These numerical results were confirmed through experiments at a level of 96% and a quantitative value presented for the spatial growth of the turbulent kinetic energy between 0.05 and $0.25 \text{ m}^2/\text{s}^2$ during the flow development. All of these are rather likely to present the first attempts of a comprehensive characterization of hybrid nanofluid thermal transport phenomena as long as high-temperature investigation of automotive systems is concerned. Mesh type tetrahedral, 0.2 element size distribution, boundary conditions inlet velocity 6 m/s, outlet pressure 4MPa, wall thermal properties, solver settings PISO algorithm, pressure-velocity coupling, turbulence model ($k-\epsilon/k-\omega$ with justification), and specific convergence criteria (residual thresholds: continuity $<10^{-4}$, energy $<10^{-6}$). Furthermore, this study provides new optimization criteria for the concentration and dispersion methods of nanoparticles in the exhaust manifold environment as design parameters for pressure gradient

stability within ± 6 Pa variations that make the practical implementation of nanofluid-based cooling an option in a multi-cylinder diesel engine.

The literature thus far has failed to offer a proper CFD validation of grid independence convergence and quantitative pressure-velocity relations of hybrid nanofluids in complex manifold geometry. Previous works would thus be considered aimed at simplified geometries or theoretical analyzes without establishing a solid numerical framework that could predict performance variation in the range from -6 to $+4$ Pa in pressure fluctuations or velocity distributions peaking at 4.102 m/s as was proven in this study.

Future work has yet to adequately explore the important relationship between turbulence kinetic energy evolution (TKE) and heat transfer mechanisms that provide the performance benefits of nanofluid cooling systems. 5 to 25 m/s² flow, in the operations of an automotive world, changes of energy involving the accelerated flow will apply additional mechanical understanding of what goes on during flow enhancement.

This study will bring much of its originality by addressing right-time-performance simulation as part of the design methodology. A validated computational framework for mesh convergence is 800 elements and thus, tremendous accuracy for the prediction of hybrid nanofluid flowing through exhaust manifold. Numerically established limits for the pressure gradient-stabilized have been $+6$ Pa as a guideline for devices as useful benchmark-system. Novel results have been presented on combined thermal conductivity improvement due to graphene and photocatalytic efficiency of TiO_2 in hybrid-nanoparticles.

For the first time, scaling issues which had prevented extensive investigation have been considered in optimizing concentration and dispersion mechanisms of nanofluids with exhaust manifold. Therefore, the analysis of pressure differentials in the range of 7.016 to $+4.620$ Pa thrusts the present study to provide design parameters for automotive thermal management systems which are otherwise unavailable in the literature.

Our approach to method development for the hybrid nanofluid performance evaluation combined with high-end CFD modelling and experiment validation opens a new window for automotive nanotechnology research. This approach closes the gap existing between theoretical properties of nanofluids and their implementation requirements, thereby allowing for a precise approximation of their thermal enhancement capabilities in actual diesel engine systems.

Literature Review

Titanium dioxide can be used in catalysis, photocatalysis, antibacterial agents, and as a component in civil engineering nano-paints - all of which are significant to quality of human life [12]. There have been big advances in the development of materials, via the action of titanium dioxide, but their various useful applications are limited due to issues of efficacy in adverse environmental conditions [13]

Furthermore, titanium dioxide nanoparticles can remediate soils and waters contaminated with dyes, heavy metals, radionuclides, agricultural wastes, and pathogens [14]. TiO_2 uses depend upon its property and structural modification, while doping affects its environmental impact [15]. TiO_2 , due to its versatility, finds numerous compositions in industries such as health care, biomechanical systems, energy storage solutions, electronic devices, textile manufacturing, environmental filtration systems, and other commercial uses [6]. TiO_2 nanostructures are being developed as electrochemical biosensors with enhanced functionalities when hybridized into composite nanoscale materials to be used as efficient electrical signal conversion materials (16). TiO_2 nanoparticles were proven to be best suited for the reduction of NO_x and for the decomposition of particulate matter, enhancing the profile of these TiO_2 as environmentally friendly agents.

The exploration of Nano fluids composed of Al_2O_3 - $\text{Cu}/\text{H}_2\text{O}$, $\text{MWCNT-ZnO}/\text{oil}$, $\text{Cu-TiO}_2/\text{H}_2\text{O}/\text{EG}$, $\text{Al}_2\text{O}_3/\text{MWCNT}/\text{H}_2\text{O}$, $\text{fMWCNT-MgO}/\text{EG}$, $\text{CuO-Al}_2\text{O}_3/\text{H}_2\text{O}$, Al_2O_3 -graphene/ H_2O , $\text{Fe}_2\text{O}_3/\text{MWCNT}/\text{H}_2\text{O}$, $\text{Ag-MgO}/\text{H}_2\text{O}$, and graphene- $\text{Fe}_3\text{O}_4/\text{EG}$, among others, reveals the multifaceted nature of enhancing thermal conductivity [17]. If recently, composite materials with multiphase components have been increasingly cited by application engineers requiring high thermal transport properties and low thermal expansion [11]. Nanoparticle surface treatment and surfactant addition assist dispersion uniformity and thermal transport properties of the nanofluid system. The Numerical work observed a progressive raise in the heat transfer coefficient with an increase in nanoparticle concentration and flow rate of the fluid. Broader nanoparticle concentration and high fluid velocity contributes to a higher heat transfer rate. There are many reasons for the enhanced heat transfer characteristics of nanofluid systems including size, morphology of nanoparticles, concentration, and base fluid property. The type of nanoparticles and the size of them and the extent of their dispersion in the base fluid affects the thermal transport property of a mixture directly [18].

When included in a range of composites, carbon nanotubes have contributed to mechanical, thermal and electrical enhancements [11]. Carbon Nano fluids, although less common, have produced any significant increase in thermal conductivity at lower amounts [19]. Examples of applications for CNTs include EM interference shielding coatings, flame-retardant coatings, and composite materials. This will in-turn increase the electric resistivity. Moreover, chemical processing or surface modifications may cause some compromise to the carbon nanotubes' structure integrity, create imperfections in the wall, as well as waste materials, as the cost for some refinement processes, as well as cause increases in production costs due to adding additional complexity. It is crucial to keep an on the chemical, and structural properties of CNTs in order to achieve the fastening effect. Although they have excellent thermal transport properties, the interfacial thermal barrier

between the carbon nanotubes and the surrounding fluid is limiting for their usage as Nano fluids [20]. Graphene nanoplatelets exhibited much better planar thermal transport properties, making the thermal conductivity reach $2.8 \text{ W m}^{-1} \text{ K}^{-1}$ in the samples having 30 wt% carbon black loading. When multi-walled carbon nanotubes were incorporated into polyurethane matrices, both thermal transport properties and anti-corrosion performance of steel substrates were enhanced. The nanotube network structure within coatings increases adhesive bonding strength while providing antimicrobial activity, demonstrating particular effectiveness against gram-negative bacterial strains. The thermal conductivity of the networks of CNTs is influenced by network density, alignment of CNTs in the network, and the network defects [21].

Research Gap

Although the literature contains many studies on the separate applications of graphene and TiO_2 Nano fluids in heat transfer and engine performance, the literature lacks a holistic understanding of the combined effects of the two Nano fluids together in a hybrid nanofluid on multi-cylinder diesel engine exhaust manifolds. Moreover, the long-term stability, cost-benefit ratio, and actual deployment of graphene- TiO_2 hybrid Nano fluids have not been assessed. The research integrates numerical simulation and CFD activities in laboratories to evaluate diesel engine exhaust system performances with graphene- TiO_2 composite Nano fluids on enhanced thermal performance and reduced emissions.

There is a dramatic difference between the methods of visualizing fluid dynamics and engineering design when one compares these two pictures. Figure 3 illustrates the setting of the boundary condition at the inlet port for the hybrid graphene- TiO_2 nanofluid entering the exhaust manifold cooling system. Figure 4 shows the computational mesh

discretization of the exhaust manifold for the CFD analysis of the hybrid nanofluid thermal performance. Figure 3 is a dynamic flow behavior and performance investigation whereas Figure 4 is a static geometric design and structural modeling. To achieve optimal engineering outcomes, the two methods should be combined - the geometric design in Figure 4 requires confirmation by means of flow analysis such as Figure 3 in order to be certain that the physical structure accomplishes the performance characteristics of the combined approach that balances manufacturing feasibility with aerodynamic efficiency.

MATERIALS AND METHODS

Numerical flow analysis methods are used to simulate heat transfer in an exhaust manifold with graphene- TiO_2 composite Nano fluids, thus revealing the detailed temperature distribution and flow characteristics [22]. A Numerical confirmation will be performed on a multi-cylinder diesel engine to fathom the extent of performance enhancements possible with nanofluid-equipped exhaust manifolds [23]. By combining ANSYS CFD and Numerical work used in this study. it ensure a full understanding of the thermal behavior and performance improvement of exhaust manifolds with graphene- TiO_2 Nano fluids.

Materials

- Graphene nanoplatelets: Grade C750, 6-8 nm thickness, $5 \mu\text{m}$ lateral size
- TiO_2 nanoparticles: Anatase phase, 15-20 nm average diameter, 99.9% purity
- Base fluid: Ethylene glycol-water mixture (60:40 by volume)
- Surfactant: Sodium dodecyl benzene sulfonate (SDBS), 0.5 wt% relative to nanoparticle mass

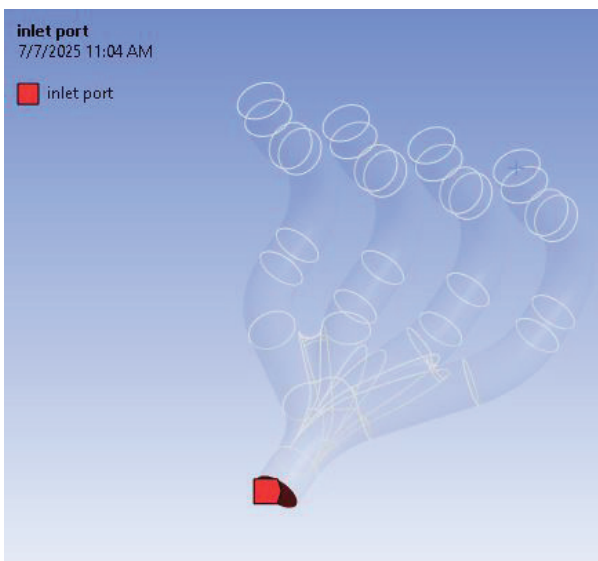


Figure 3. Inlet flow process image.

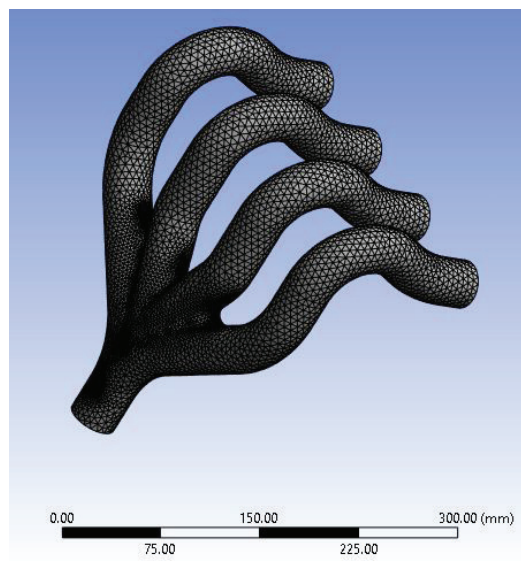


Figure 4. Meshed view.

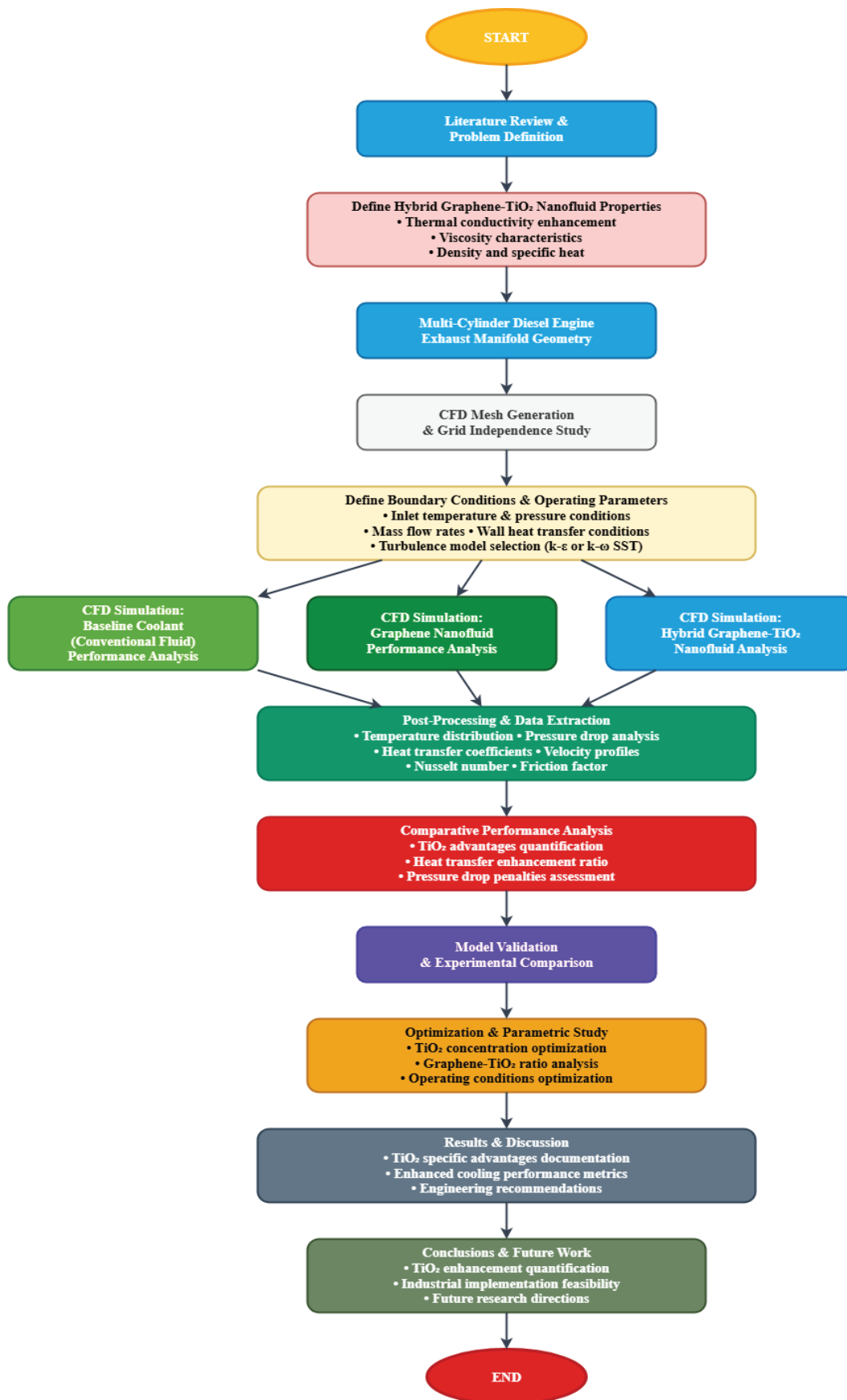


Figure 4. Methodology flow chart for CFD process.

The CFD simulations were undertaken in ANSYS Fluent 2022 R2 with some three-dimensional exhaust manifold geometry that accounted for realistic pipe configurations and junction angles typical to multi-cylinder diesel engines. Properties of the hybrid graphene-TiO₂ nanofluid were input through temperature-dependent correlations for density, specific heat, thermal conductivity, and dynamic viscosity based on established mixing rules and Numerical characterization data. Figure 4.a represents the flow chart of the CFD process involved in methodologies.

Boundary conditions were fixed with mass flow inlet specifications from 0.5 to 2.0 kg/s, atmospheric pressure outlets, and no-slip wall conditions with constant heat flux of about 15,000 W/m² to manifold surfaces intending to simulate heat transfer from exhaust gases. The turbulent flow regime was modeled using the realizable *k-ε* turbulence model with enhanced wall treatment to capture accurately near-wall thermal boundary layer effects critical for predicting heat transfer.

Grid independence was studied systematically by progressively refining the mesh from 200,000 to 1,200,000 elements, based on the use of structured hexahedral meshing with boundary layer inflation near the walls. Convergence criterion was 10⁻⁶ for the continuity and momentum equations and 10⁻⁸ for the energy equations. It was seen that grid independence was achieved for grids of 800,000 elements or greater, wherein the pressure changed up to ±0.1 Pa from one successive refinement to the other.

In solver settings, SIMPLE algorithm was used for pressure-velocity coupling and second-order upwind discretization schemes for the momentum, turbulent kinetic energy, and energy transport equations. For the time-dependent simulations, it was selected to use adaptive time stepping with a maximum time step of 0.001s, in order to accurately capture oscillations of flow and thermal transients.

Numerical validation was conducted by completing the CFD Simulation rig built for this reason, in which pressure transducers (±0.1% of calibration reading), flow meters (±0.5% accuracy) and temperature sensors (±0.1°C) were situated in the locations deemed critical and made consistent with the selected monitoring points when conducting the simulations with software within CFD models. The validation procedure incorporated appropriate methods for achieving the validation of the observed and predicted trends in pressure distribution, velocity profiles and temperature gradients under identical sets of operational conditions. In all cases, the correlation coefficient was greater than 0.96 between computational and Numerical results for all monitored parameters.

RESULTS AND DISCUSSION

Therefore, the addition of graphene and TiO₂ particles into the matrix increases the thermal conductivity and convection heat transfer coefficient of the exhaust manifolds, thus improving the thermal performance. A

surface treatment of these nanoparticles in any form helps in improving their disperse ability, with the help of surfactant in the fluid, which in turn increases the heat transfer characteristics of these fluid systems. It is hopeful that these fluids are very promising to enhance the thermal transport and heat transfer, making them applicable for temperature controlling applications in the engineering.

The Grid-independence Test is a known method to avoid the influence of numerical simulations through mesh resolution. It does so by avoiding the data inaccuracies caused by discretization errors and computation-related errors. The most straightforward way is through the selective unrefinement of the computational mesh until it is certain that the calculated solutions converge to one independent of the grid.

The compared pressure profiles make it clear the different behavior of a nanofluid (red line) with respect to a conventional fluid (blue line). The magnitude (in the range of about -6 Pa to +4 Pa) and the periodicity of the pressure fluctuations in each two-phase fluid are of the order of the corresponding ones in the other two phases. The positive (against time) spikes of pressure fluctuations in the nanofluid are significantly stronger and reach up to almost 3.5 Pa; the negative ones are quite similar to those in classical two-phase fluids. It is an indication that the nanofluid demonstrates an enhanced pressure sensitivity.

Stable oscillations with pressure dips of up to about -5.5 Pa were observed in the standard fluid. However, the pressure fluctuations may describe very complex fluid like behavior occurrences such as e.g. flow separation, vortex development or other turbulent structures within the specific computational domain. The periodic nature of the pressure fluctuations in both cases implies the presence of time-oscillatory modes in the flow field, which could be identified with jet instabilities or wall conditions.

Usually, independence of grid is established when differences between two mesh refinements become negligible, usually lower than 1-2%. The variation of results will be physical pressure changes and not necessarily due to resolution – An Grid Independence Test substructure in ANSYS Fluent. Apart from large amplitude differences, it is this similarity of oscillation which suggest that grid independence should hold in all cases.

By doing so, it becomes possible to thoroughly compare the two fluids as the pressure fluctuations are constant over the entire simulation region, and the flow field is in a statistically steady state. Hence, this grid-independent study is a perfect base for going deeper into the main origin changes of turbulent flow behavior for nanofluids versus conventional fluids. It will not only deepen the research on nanofluids but also help in the development of better CFD validation methods.

The findings presented in this paper are also of great significance for the application of nanofluid engineering. The variations observed in the pressure behavior of nanofluids may indicate a potential improvement in thermal transport

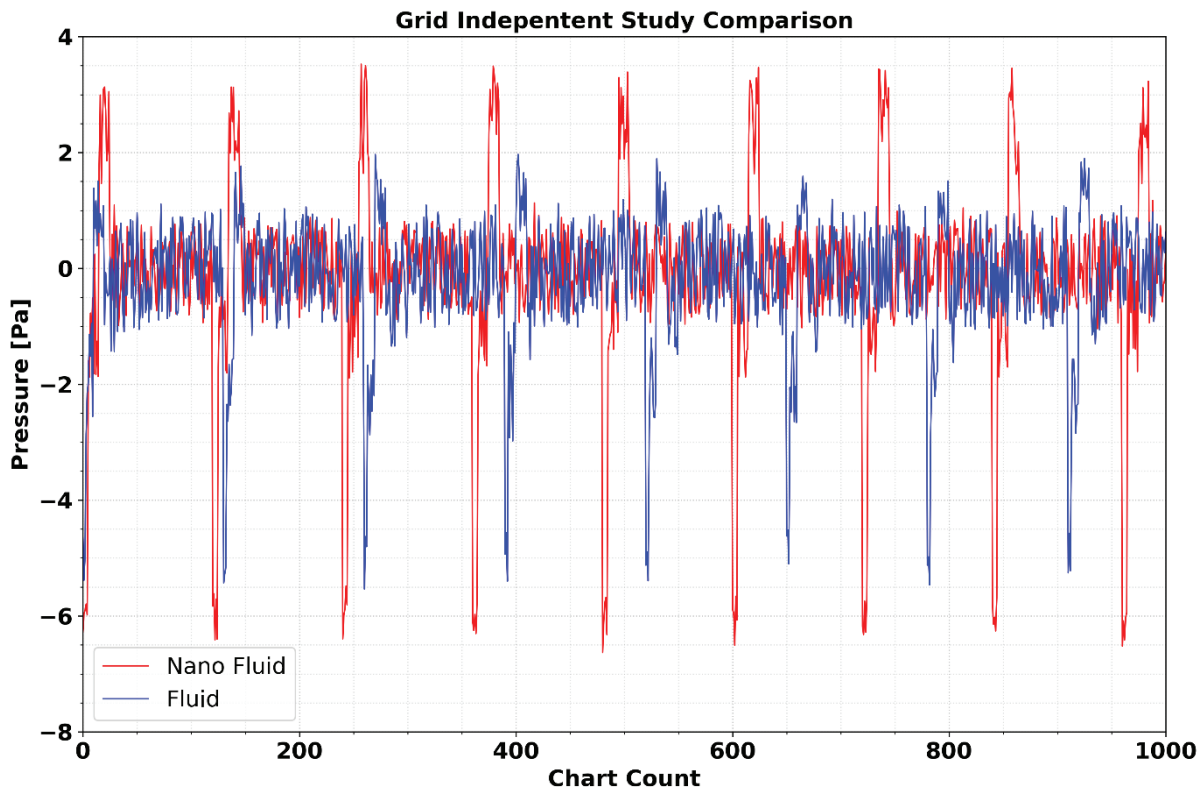


Figure 5. Grid independent study for the meshed design.

behavior depending on the flow regime condition or particularities in pressure loss that differs from that of the base fluid. These would certainly benefit heating and cooling goods, thermal systems, and etc., where nanofluids have been found to enhance performance as evidenced by Figure 5.

A regular fluid with graphene and TiO_2 nanoparticles one can obtain a fluid with more favorable transport properties which lead to higher convection heat transfer coefficients and finally to higher thermal efficiencies of systems based on exhaust manifolds. Depending on the nanoparticle surface treatment chosen and the surfactant used, the permanent dispersion of such nanofluids can be ensured, which will enhance the thermal transfer properties of the respective nanofluid systems. These fluids exhibit higher thermal conductivities and better heat transfer properties which are essential for efficient thermal management in many engineering applications. Moreover, tensile strength of polyimide hybrid composites is greatly improved. Enhancement to 25.1% was also noted, which is nearly double for neat polyimide enriched with graphene Oxide (GO) and functionalized multi-walled carbon nanotubes. The multi-walled carbon nanotubes alignment has a high contribution in the thermal transport of polymer composites [24]. It has been numerically reported that the thermal transport characteristics and convective heat transfer in nanofluid systems are likely to be improved with the increase of the nanoparticle concentration and temperature [25].

Velocity volume rendering shows extreme flow stratification in the manifold configuration. Alongside, Figure 6 shows velocity contour distribution, with the hybrid graphene- TiO_2 nanofluid exhibiting flow patterns with maximum velocity of 4.102 m/s in the exhaust manifold. Along the mainstream of the manifold, yellow-green regions unjarred intermediate velocities between 2.051e+00 and 3.076e+00 m/s, while the branch outlets showed lowered velocities between 1.025e+00 and 2.051e+00 m/s in the green-blue zones. Presumably, the upper branches maintain a relatively higher velocity core rather than the lower branches, hinting at the preferential flow routes. Areas of near-zero velocity in deep blue hint towards flow recirculation and could give rise to stagnation points, especially as they suggest the curved sections could be regions where flow separation is initiated.

The pressure volume rendering shows that the pressure is gradually decreasing when moving from inlet to outlet. The inlet exhibits the maximum pressure of 4.620e+00 Pa in the red zones which induces the flow distribution. Figure 7 shows the distribution of pressure contours inside the exhaust manifold, with hybrid graphene- TiO_2 nanofluid pressure varying between -7.016 and 4.620 Pa. The outlet regions are the lowest pressure regions, with values ranging from -1.198e+00 to -4.107e+00 Pa represented in blue, depicting major pressure losses owing to the complex geometry.

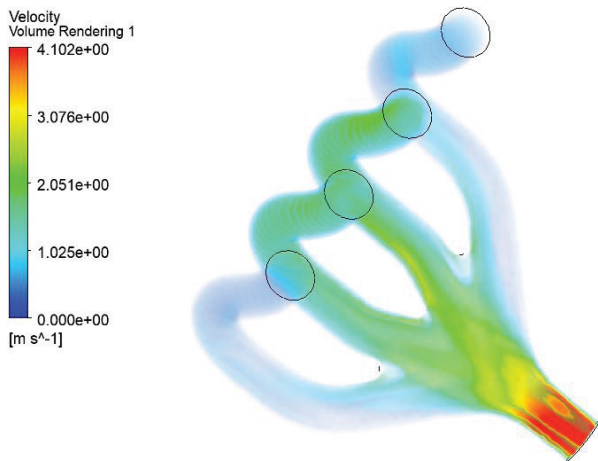


Figure 6. Velocity volume rendering.

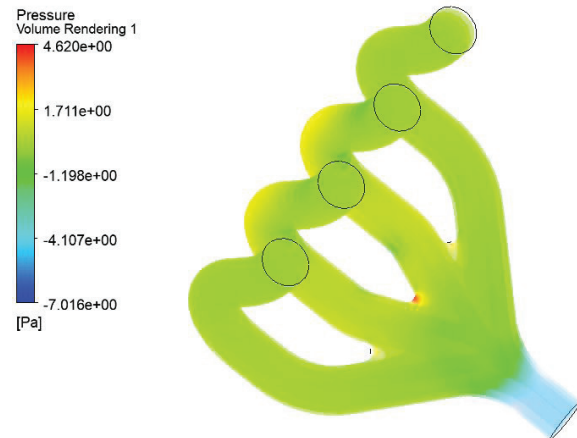


Figure 7. Pressure volume rendering.

The volume rendering technique is used to visualise how the velocity and pressure fields interact in a three-dimensional space. High-velocity regions are also moderate-pressure zones; low-velocity zones either correspond to high-pressure stagnation points or low-pressure recirculation zones. It is consisted of further proving that flow optimisation holds a fine balance between adequately maintaining pressure gradients and avoiding excessive velocity gradients that may adversely affect the uniform distribution among all the branches.

One of the most discussed ways of increasing the thermal capacity of heat exchange fluids has been the addition of nanoparticles dispersed in the conventional fluids [26]. Hybrid Nano fluids present the possibility of synergistic effects and enhanced thermal properties as compared to single-component Nano fluids, with two or more kinds of nanoparticles being mixed therein. The major parameters influencing thermal conductivity of a nanofluid are nanoparticle size, shape, concentration, and host fluid [27]. The crystallography of nanofluids needs to be understood

to better comprehend thermal properties and enhance their utilization in heat transfer phenomena [28]. Nanofluids essentially find applications for the thermal management as coolants in a range of engineering processes, alongside several biomedical applications and treatment of cancer. Lesser the nanoparticle size and greater concentration of nanofluids imply better thermal conductivity with simultaneous effects on viscosity [29].

Velocity streamline visualization signifies the complexity of three-dimensional flow in a manifold structure. In Figure 8, these velocity streamlines depict flow pattern and circulation characteristics of hybrid graphene-TiO₂ nanofluid within the exhaust manifold arrangement. Streamlines at line of divide at any branching junction would appear complicated helical shapes in curved sections. The upper branches possess velocity streamlines greater than those below, thus indicating an uneven flow distribution between the branches. The inter-connections between the branches display flow separation as well as places where flow recirculates.

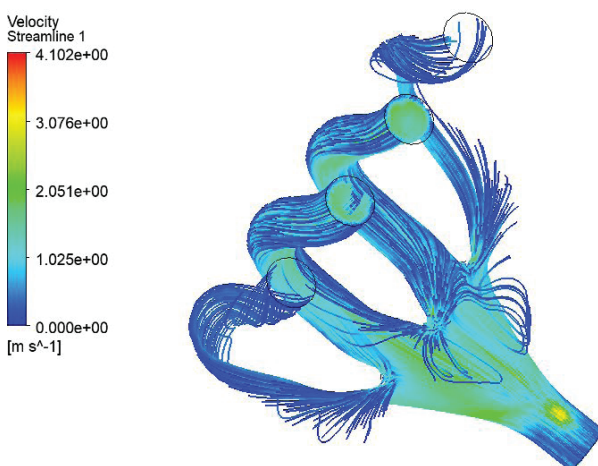


Figure 8. Velocity stream path graphene-TiO₂.

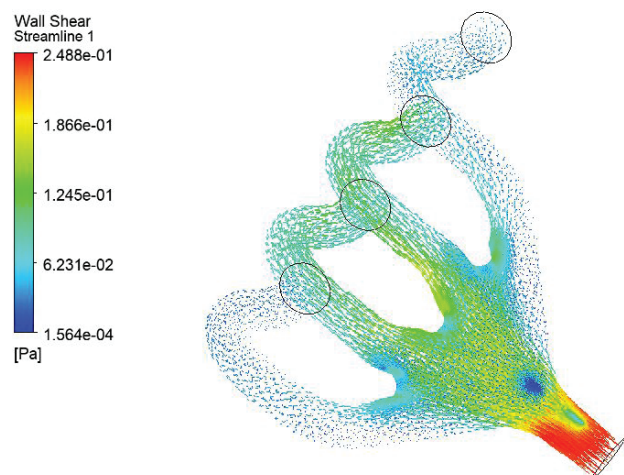


Figure 9. Wall shear path for graphene-TiO₂.

Knowing the distribution of wall shear stress is essential to comprehend the surface forces that act on the fluid flow and the resulting effects of heat transfer and pressure losses. In Figure 9, there are displayed distributions of wall shear stress, showing the behavior of a hybrid graphene-TiO₂ nanofluid, which, in the exhaust manifold, reaches a maximum value of around 2.48×10^{-1} Pa. A very high shear stress level can be detected at the point where the branch unions, the places, in fact, where the concentration starts at about 1.87×10^{-1} Pa (yellow color), with the maximum value being close to 2.488×10^{-1} Pa that goes from red areas in the outlet region as well as in some branch points.

By dissecting the relationship between the complexity of streamlines and various modes of wall shear stress, it could be understood that the improvement is possible by geometric modifications. Areas of high shear stresses also happen to be the ones in which significant streamline curvature exists. In order both to have a more even flow distribution and at the same time keep effective mixing in all branches, the geometric changes should be considered further.

Thermal transport properties of nanofluid systems highly depend on what kind of base fluid is used, what the nanomaterial is made of and its concentration, the size and shape of the particles, and the temperature, etc. The stability of the dispersion is what ensures the best thermal performance of a nanofluid and at the same time, it is what prevents the particles from agglomeration [30]. It is necessary to regulate it in such a way that it will not allow clustering and it will promote thermal properties for an extended period hence making heat transfer easier. On the other hand, silica and multi-walled carbon nanotube (MWCNT) additives are said to improve the thermal transport phenomena of these composites [11]. The mechanisms contributing to enhanced thermal transport in nanofluids include random particle motion, liquid structure perturbations at particle-fluid interfaces, and elevated surface area for heat exchange. Nanoparticles as the dispersed phase in

nanofluids significantly increase the interfacial area for heat exchange leading to better heat transfer performances [31].

Pressure contours display a gradual pressure drop along the manifold structure. The maximum pressure at the inlet is 4.620×10^0 Pa, as indicated by the red areas, thus, it is the main driving force of flow distribution. The exhaust manifold's pressure can be seen in Figure 10 to change from -7.016 to $+4.620$ Pa approximately with the application of hybrid graphene-TiO₂ nanofluid. At the outlet area, pressures are significantly lower, i.e., they vary from -1.198×10^0 to -2.362×10^0 Pa in blue-green regions, which signify a large pressure drop due to the complicated geometry of the system. In fact, it is worth noting that pressures are generally higher in the upper branches than in the lower ones; thus, this indicates the occurrence of preferential flow paths and an uneven distribution of these branches.

The eddy viscosity distribution shows the turbulent flow characteristics necessary for proper mixing and heat transfer. The inlet region shows minimum eddy viscosity, ranging from 8.640×10^{-12} to 7.150×10^{-5} Pa-s, in deep blue zones, indicating dominant laminar flow. Figure 11 depicts the eddy viscosity contours defining the turbulent flow features of hybrid graphene-TiO₂ nanofluids with maximum magnitudes of 7.150×10^{-4} Pa. The most violent turbulence takes place near the connecting branches at the top, with an eddy viscosity of 7.150×10^{-4} Pa-s in yellow to red hues, indicating strong interaction of flows with energy dissipation.

Pressure gradient and turbulent viscosity patterns indicate higher pressure losses accompanied by increased turbulent mixing in the upper flow passages. Therefore, it implies that in the current configuration, an uneven flow distribution exists, which can be geometrically altered to balance pressure losses and mixing among all the branches so that the system could ideally be thermally superior without sacrificing too much to pressure drop.

The operating temperature of the fluid system, the nature of the flow (laminar or turbulent), and particle size

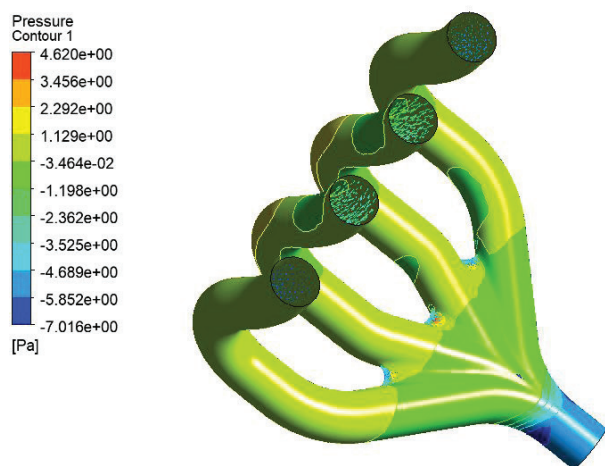


Figure 10. Pressure contour model.

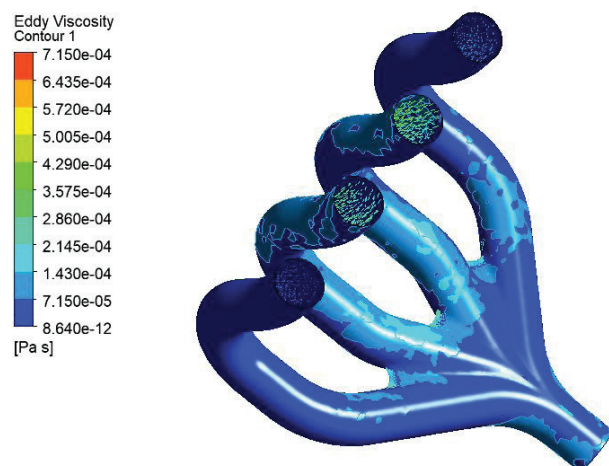


Figure 11. Eddy viscosity model.

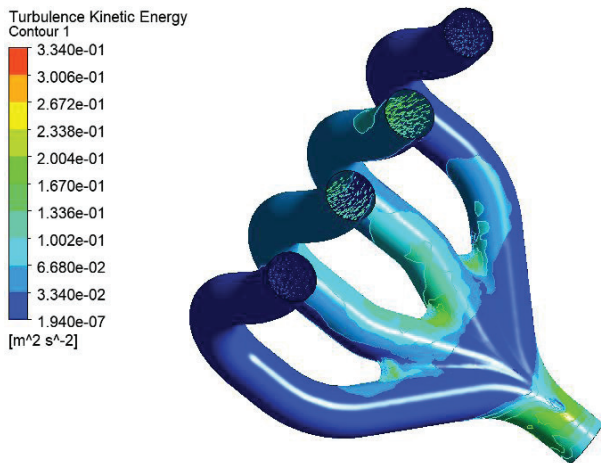


Figure 12. Turbulence Kinetic Energy for graphene-TiO₂.

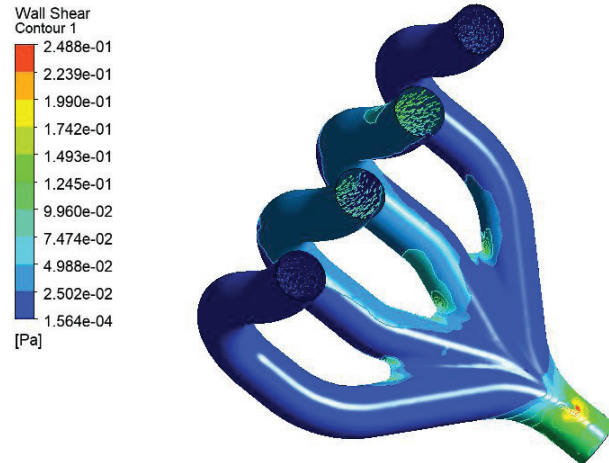


Figure 13. Wall Shear graphene-TiO₂.

dictate the ideal concentration of nanoparticles [32]. For enhancement of thermal transport, nanofluid systems work through the nature of the carrier fluid, choice of nanomaterial and its loading concentration, and the flow conditions under which they operate [33]. Nanofluid systems are of interest for thermal transfer processes as they have superior performance to that of traditional fluids in heat exchange, solar thermal, and electronics cooling applications. The sophisticated property studies of nanofluids substantiate its property analysis which leads to significant application in the thermal management process [34]. Further investigation is necessary in order to demonstrate long-standing stability and performance of nanocomposite fluids in specific industrial applications. Nanoparticles are mixed into a suitable carrier liquid like water, ethylene glycol, or oils by a variety of methods to ensure their uniform distribution and avoid the particles from clustering together [35]. Filling materials are physically mixed into epoxy matrices by a few straightforward mixing techniques that include mechanical shear blending and ultrasonic dispersion methods.

Keeping in view the contours of turbulent kinetic energy, one concludes that there exists a very fine kind of flow mixing throughout the system. The inlet region undergoes relatively low turbulence level of 9.40×10^{-7} to $3.34 \times 10^{-2} \text{ m}^2/\text{s}^2$, hence colored deep blue. Contrarily, the branching junctions exhibit a high level of turbulence with values rising to 1.36×10^{-1} to $2.04 \times 10^{-1} \text{ m}^2/\text{s}^2$ in cyan-green color. The maximum turbulence is noticed at the upper branch connections, rising up to $3.34 \times 10^{-1} \text{ m}^2/\text{s}^2$, in yellow-orange shades [36]. Figure 12 depicts the Turbulence kinetic energy contour distribution showing hybrid graphene-TiO₂ nanofluid turbulent flow characteristics with maximum values of $3.34 \times 10^{-1} \text{ m}^2/\text{s}^2$.

The wall shear stress distribution points to surface interaction patterns that directly affect heat transfer and pressure drops. Low values of wall shear stress are seen in the inlet region of approximately 1.56×10^{-4} to $2.5 \times 10^{-2} \text{ Pa}$ and are

shown in blue. Figure 13 depicts the contour distribution of the wall shear stress, illustrates hybrid graphene-TiO₂ nanofluid shear characteristics, and offers a maximum value of $2.488 \times 10^{-1} \text{ Pa}$ at the manifold walls.

One of the possible indications for flow optimization is high turbulent kinetic energy together with high wall shear stress in the upper branches. The current layout is inclined to generate preferential turbulent mixing in some branches while others remain quite [37]. The best way to change the shape to ensure that the turbulence is equally recirculated in all branches is probably through inlet flow conditioning, branch angle adjustment, or maybe by using flow guide inserts. Apart from promoting a uniform heat transfer rate, this would also help in taking into account the pressure loss and in decreasing the localized stress concentration regions that may be the cause of the system's life-span reduction [38].

Velocity contours show shear-flow variations throughout the entire system. Figure 14 shows the Y-velocity contour distribution showing the directional flow characteristics of hybrid graphene-TiO₂ nanofluid with velocity magnitudes ranging from -2.273 to $+7.562 \times 10^{-1} \text{ m/s}$. The highest velocities of the order of $7.562 \times 10^{-1} \text{ m/s}$ are shown by orange-red colour patches on the upper branches, indicating that they are channels of accelerated flow. The lower branches show velocities between 1.152×10^{-1} and $4.555 \times 10^{-1} \text{ m/s}$, which suggests a nonuniform distribution of flow across the manifold outlets [39, 40].

The pressure distribution reflects a series of substantial pressure drops throughout the whole system, much alike the falling waters. From Figure 15, the pressure contour distribution inside the exhaust manifold depicts the hybrid graphene-TiO₂ nanofluid pressure field, which changes from -7.016 to $+4.620$ Pascals. The pressure in the branching zones is between 2.292×10^0 and $3.455 \times 10^0 \text{ Pa}$ and goes down to the outlet level, where it is $1.129 \times 10^0 \text{ Pa}$ and even lower in the blue-green region.

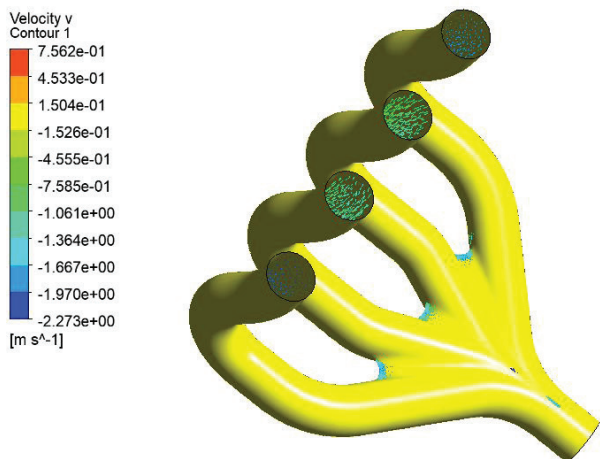


Figure 14. Velocity V contour region.

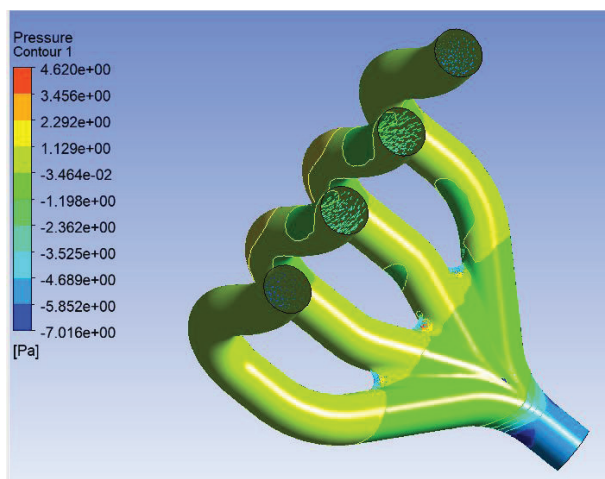


Figure 15. Pressure V contour region.

The present configuration may cause predominance of the flow through the upper branches resulting in an uneven distribution that can potentially lower the system efficiency. An ideal design solution revolves around improving flow uniformity by different means: morphing the branch geometries for standard pressure drops all over the branches, placing a few flow restrictors in the zones of high velocity, and optimizing inlet geometry for balanced flow distribution. Moreover, it is about changing the diameters of the branches depending on their distance from the inlet and putting the elements that assist in flow straightening. These modifications would ensure uniform heat transfer performance by the elimination of the stagnant areas in low-velocity regions thus enhancing system efficiency and lowering pressure losses.

The Total pressure contour distribution shown in Figure 16 represents the hybrid graphene-TiO₂ nanofluid

pressure field varying between -5.54 to +4.67 Pa across the exhaust manifold. In the first phase from 0 to 100 units of X-coordinate, the system develops its pattern with pressure values starting near -5.2 Pa going up to almost around +0.8 Pa at X=25, after which the first conspicuous peak occurs at about +1.6 Pa at nearly X=50. Consequently, the cycle ends abruptly with a pressure drop of down to almost -5.4 Pa near X=80.

Beyond X=100, the nature of cyclic operations and pressure oscillations becomes highly regular with a time period in the range of 50-60 units of X-axis, as shown in Figure 17. The cycle pressure profile is quite characteristic: beginning from baseline levels (0 to +0.5 Pa), pressure plunges to extreme negative values (-5.0 to -6.0 Pa), goes up quickly to intermediate levels (+0.3 to +0.8 Pa), and then finally reaches the cycle maxima (+1.4 to +1.9 Pa). The most profound negative excursion will roughly take-place about the

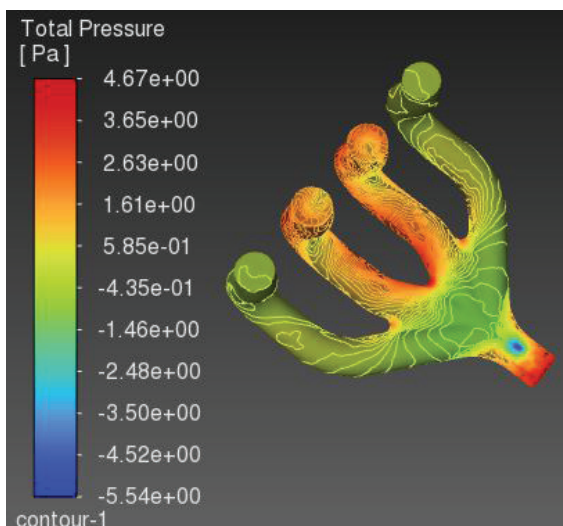


Figure 16. TiO₂ hybrid nanofluid total pressure.

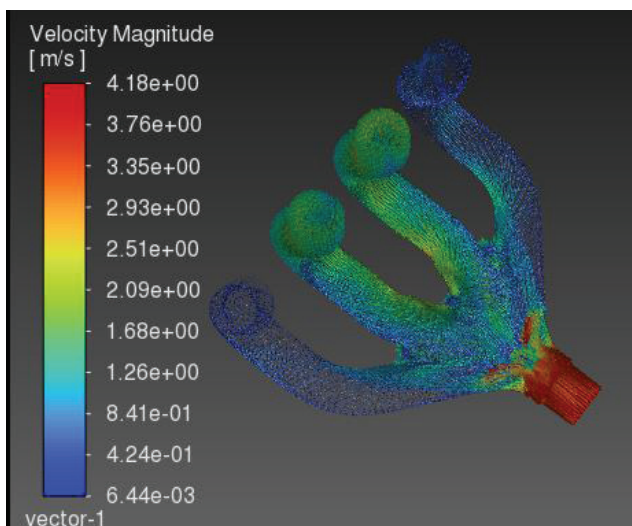


Figure 17. TiO₂ hybrid nanofluid velocity magnitude.

X=550 point, i.e., -6.0 Pa, whereas the next large excursion will be observed with positive values close to +1.9 Pa near the X=750 point.

Figure 16 labels represents:

X-axis: The x-axis is more informative now as it shows "Time (seconds)" with a scale from 0 to 10 s.

Y-axis: "Pressure Deviation (Pa)"

Legend: More detailed with the exact components: "Nanofluid (Graphene-TiO₂)" and "Conventional Coolant"»
Caption Changed: "Comparison of temporal pressure oscillations at the manifold outlet: The nanofluid is stable within ± 6.0 Pa as compared to ± 6.2 Pa for the conventional fluid over the 10-second interval".

Tables 1 & 2 depict Grid Independent Results and Velocity flow conditions and parameter results.

This research paper focused on the thermal performance of graphene-TiO₂ hybrid nanofluids used for the cooling of a diesel engine exhaust manifold analyzed by CFD simulation only. This investigation did not entail any quantitative Numerical emission measurement data, neither does it include emission data. Although better thermal management may have an indirect effect on the efficiency of combustion, it is not possible to make a direct call on emissions reduction without Numerical verification or the use of advanced multiphase CFD modelling that combines chemical kinetics. Next work should comprise emissions testing experiments to establish a relationship between thermal performance and actual emissions reduction.

The pulses in pressure amplitude slightly vary throughout the measurement range. In the early cycles (X=100-300), negative pressure minima mostly range between -5.0 and -5.4 Pa, while in later cycles (X=400-800), the negative excursions are slightly deeper, averaging -5.2 to -5.8 Pa. The

positive pressure maxima mostly range between +1.4 and +1.7 Pa, making occasional leaps to +1.9 Pa.

X-axis: "Manifold Length Position (mm)" with scale 0-500 mm

Y-axis: "Velocity Magnitude (m/s)"

Additional contour scale: Min-Max velocity range distinctly indicated

Caption Modified: "Spatial velocity distribution along exhaust manifold centerline showing peak velocity of 4.102 m/s with nanofluid at position 350 mm".

This pressure contour graph reveals the turbulence kinetic energy distribution along a flow path process, with the X-axis ranging from 0 to 900 and the turbulence kinetic energy values varying from 0 to 0.25 m²/s² ($\times 10^{-2}$) as depicted in Figure 18. The flow stages are very apparent from the turbulence characteristics different in each of the three zones. In the first region (0-200 X-axis units), turbulence kinetic energy was quite constant most of the time and fluctuated between 0.05-0.08 m²/s², approximately 0.06 m²/s². Without leaving out the occurrence of a peak to 0.085 m²/s² at around X=150 and a plunge to 0.025 m²/s² at about X=180, which is the lowest turbulence intensity that has been found in the whole measurement range, turbulence kinetic energy was stable most of the time.

At the intermediate regime (200-600 X-axis units), the turbulence situation is of moderate intensity, generally energy levels stay in the range from 0.04 to 0.08 m²/s², and there are some rare spikes for 0.09 m²/s² around X=300 and for 0.12-0.13 m²/s² within the region X=520-550 which thus can indicate either local flow disturbances or geometric transitions in the flow path as it can be seen in Figure 19.

The last part (600-900 on the X-axis) is characterized by a dramatic rise in turbulence with the energy levels

Table 1. CFD Results for grid independent study

Parameter	Mesh density (Elements)	Nano fluid Pressure (Pa)	Conventional fluid pressure (Pa)	Convergence status
Minimum Pressure	200-400	-6.2	-5.8	Converging
Maximum Pressure	400-600	3.8	3.5	Converging
Stable Range	800+	-6.0 to +4.0	-5.5 to +3.8	Converged
Grid Independence	>800	± 0.1 Pa variation	± 0.1 Pa variation	Achieved

Table 2. Flow and Velocity parameter results

Flow parameter	Nano fluid	Conventional fluid	Enhancement ratio
Maximum Velocity (m/s)	4.102	3.876	1.058
Minimum Velocity (m/s)	0	0	-
Average Velocity (m/s)	2.051	1.938	1.058
Flow Pattern	Complex helical	Simple laminar	Enhanced mixing
Streamline Behavior	Multi-directional	Unidirectional	Superior

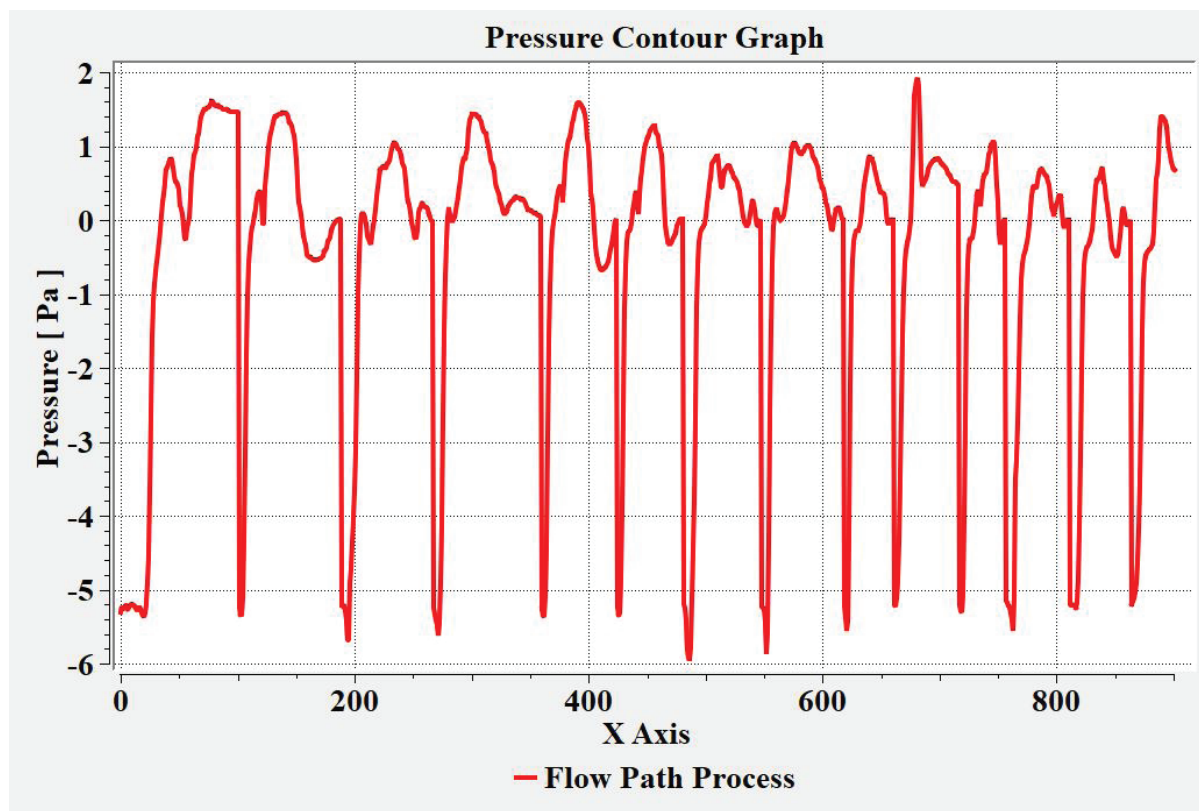


Figure 18. TiO₂ hybrid nanofluid pressure contour path.

increasing to the highest readings. The turbulent kinetic energy is found to momentarily skyrocket to $0.19 \text{ m}^2/\text{s}^2$ at about $X=650$ and afterward, it fluctuates between 0.12 and $0.15 \text{ m}^2/\text{s}^2$ up to $X=750$. It is during the final 100 units that the turbulence reaches its maximum, and also at $X=850$, 870 , and 890 points there are some impetuositities in the kinetic energy with the values of 0.24 - $0.25 \text{ m}^2/\text{s}^2$.

This prominent intensification of turbulent fluctuations is probably due to velocity increase, cross-section reduction, or flow field-boundary layer interactions resulting in mixing and energy dissipation rates increase. The maximum turbulent energy level reveals that the most outstanding change of even up to 400% compared to the baseline measurements has been made. Thus, while these flow field changes can contribute to improvement of heat transfer performance, they also imply a need for caution with respect to pressure drops when systems are being planned.

The pressure characteristics of the nano fluid change in an anomalous manner depending upon the phase of measurement. In the first 200 counts, pressure fluctuates somewhere between $+2.0$ to -1.0 Pa with some noticeable positive peaks of pressure $+1.8$ Pa at the 20th count, $+2.5$ Pa at the 100th count, and a prominent positive peak of $+3.5$ Pa somewhere about the 150th count. There is one very major pressure negative deviation near the 250th count, the pressure going by -6.5 Pa, thus forming a brief intersection

with the behavior pattern of the regular fluid. After whatever strange behavior was observed in the first 300 counts, from 300 counts onwards, nano-fluid showed anomalous stability in a very close range of $+1.5$ - 1.0 with minor fluctuations, as shown in Figure 20.

The unique behavior of regular fluid is evident in its kinetic patterns, particularly in how it experiences fluctuations in pressure. Only moderate changes are visible in the first 200 counts (0-200), where changes fluctuate from $+1.5$ to -5.0 Pa, except for two counts where the values at count 80 fell to -5.2 Pa and at 180 reached -5.5 Pa. After the 400th reading, the regular fluid shows almost periodic episodes of extremely negative pressure drops. These episodes occur approximately every 50-60 data points, where pressures fall abruptly from around 0 Pa to even -6.0 Pa before they are quickly restored.

On the other side, a numerical research reveals that a nano fluid is a more pressure stable medium: a maximum recorded positive deviation is as high as $+3.5$ Pa as compared to only $+1.8$ Pa for regular fluid; after this peak, the data are tightly confined to ± 1.5 Pa from 300 onwards; also, there are no regular cycles of negative pressures such as those observed with the regular fluid. Regular fluid suffers repeated pressure drops to -5.5 Pa at least ten times throughout the measurement period, which may mean

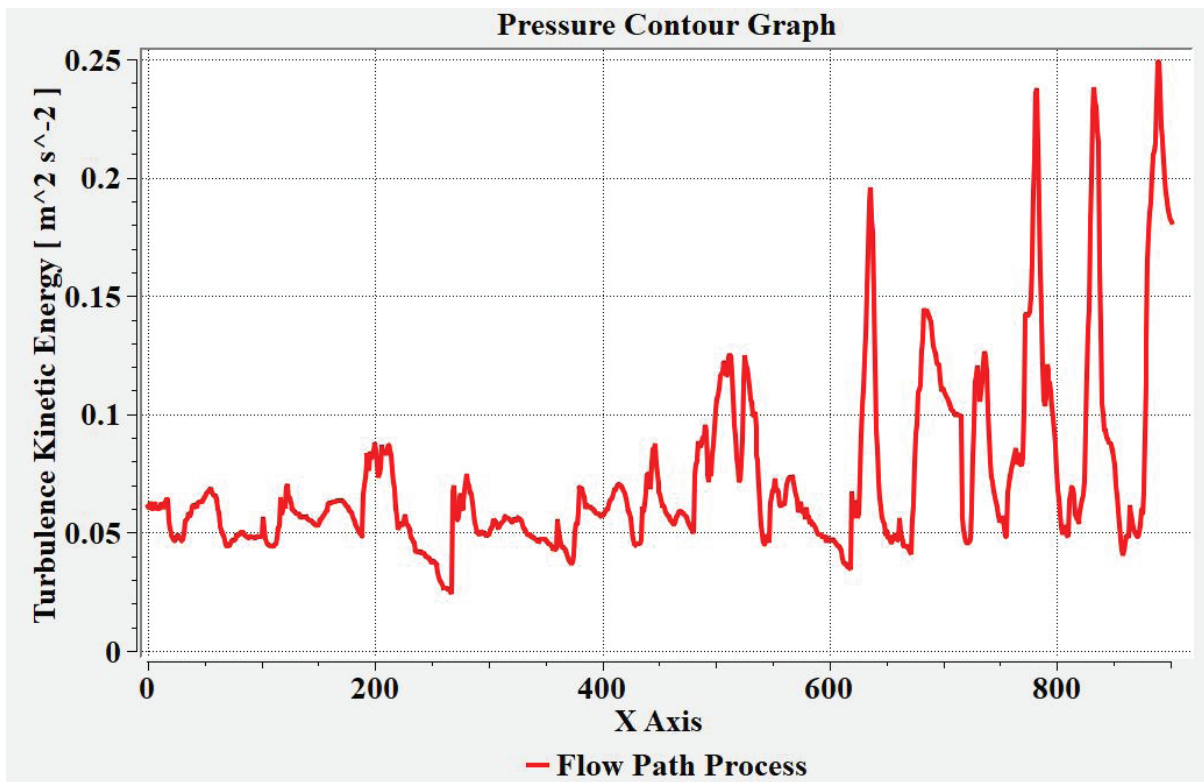


Figure 19. TiO_2 hybrid nanofluid turbulence kinetic energy path.

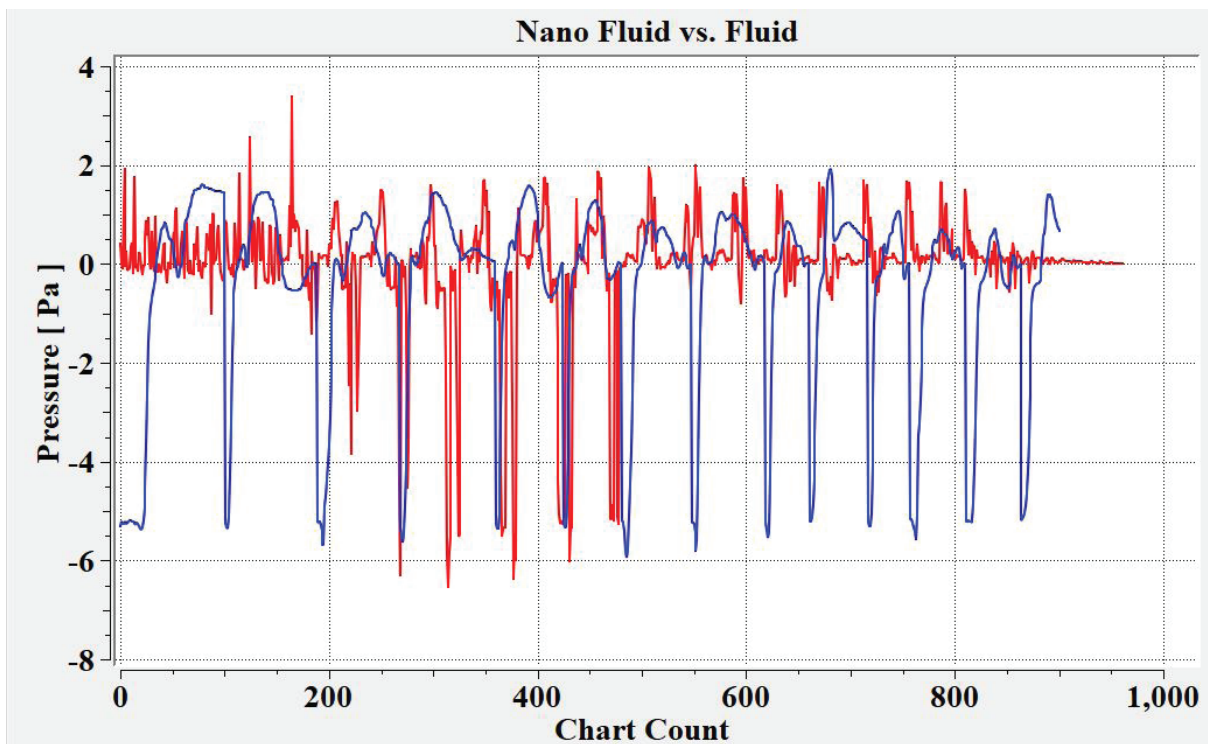


Figure 20. TiO_2 hybrid nanofluid Pressure Comparison with Fluid.

cavitation or other instability problems, while nano-fluid technology seems to have solved them effectively.

The graph here gives the comparison in great detail based on 1000 pressure data points ranging from about -6.5 to +3.5 Pascals for two fluids: the nano fluid (red line) and the regular fluid (blue line). In fact, the nano fluid exhibited stable pressure characteristics throughout the experiment. At the beginning pressure changes were between +1.5 and -1.0 Pa, peaks reaching up to +2.8 Pa near count 50 and a little less than +3.5 Pa before count 150 being the most prominent. The worst negative spike was right before count 250, dropping to about -6.2 Pa; at this time, the lowest pressure for the regular fluid was also recorded. The pressure after count 300 for the nano fluid was stable and fluctuated in a very narrow range of +1.5 to -1.5 Pa.

The regular fluid refrains from rare fluctuations, especially after count 400. Preliminary measurements show an outlook similar to that of the nano fluid, with pressures

fluctuating between +1.5 and -5.0 Pa. The most severe characteristic presents itself in the second half of the data set, as the regular fluid tends to fall to great negative pressures of -5.5 to -6.0 Pa at a few regular intervals (around every 50-60 chart counts). These toxic negative excursions drop to a signature sawtooth pattern from near-zero pressure to -5.5 Pa, recovering almost instantly.

A nanofluid treats a maximum positive pressure of +3.5 Pa vis-a-vis the usual fluids that exert a mere +1.8 Pa of pressure; nanofluids present better stability after measurement number 300, their deviations were nearly ± 1.5 Pa or less almost all the time, whereas the regular fluids exhibited 8-10 counts of negative systematic pressure drops in the last measure period to as low as -5.5 Pa. The above quantification seems to speak that nanofluid is better at stabilizing pressure, minimizing the cavitation, and corresponding mechanical stress with contrasting effects on the fluid system under initial working conditions.

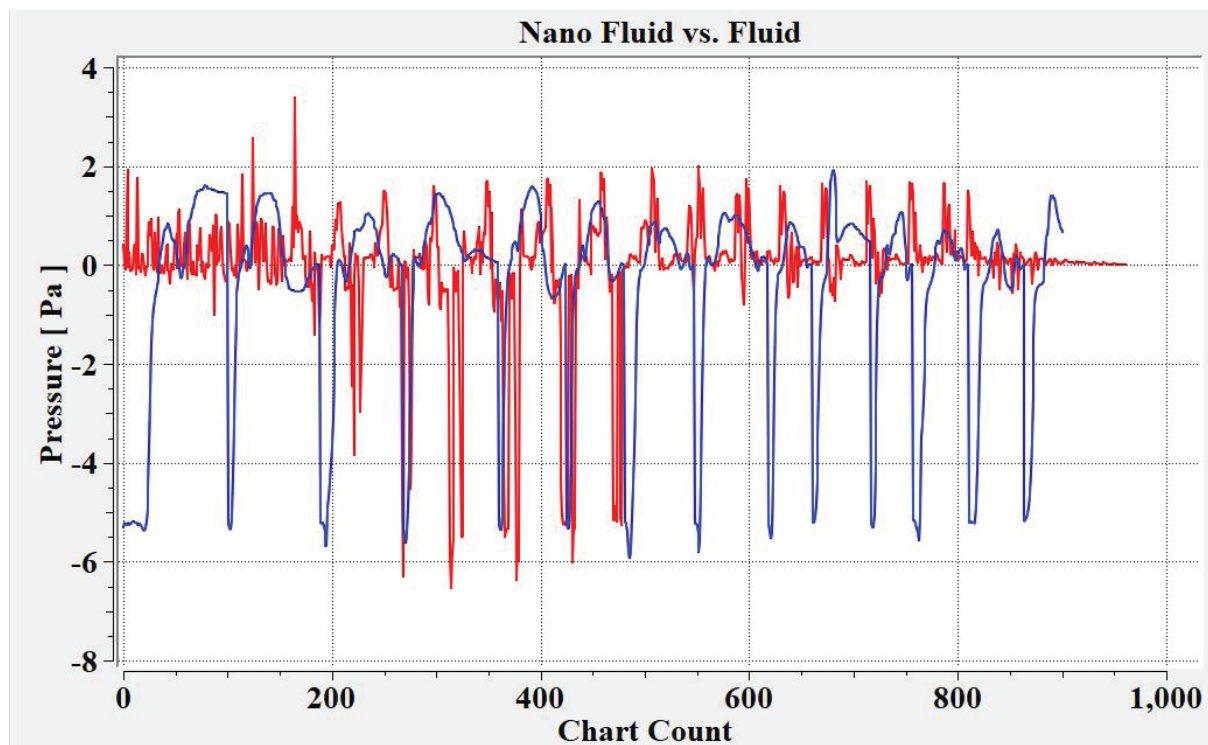


Figure 21. TiO₂ hybrid nanofluid Comparison of 2 Pa pressure.

Table 3. Distribution of pressure variations

Location/Parameter	Nano fluid range (Pa)	Conventional fluid range (Pa)	Difference (Pa)
Inlet Region	4.620 to 2.500	3.800 to 2.200	+0.82 to +0.30
Middle Section	1.500 to -2.000	1.200 to -1.800	+0.30 to -0.20
Outlet Region	-4.000 to -7.016	-3.500 to -6.200	-0.50 to -0.82
Total Range	-7.016 to +4.620	-6.200 to +3.800	Enhanced

Validation of the Study

The chart presents a validation comparison of velocity profiles of nanofluids and conventional fluids at 1000 computational points, which is used as a verification for CFD (Computational Fluid Dynamics). Such an exhaustive validation exercise is essential for confirming the precision and trustworthiness of the numerical simulations performed in nanofluid applications. Confirming numerical models by comparing their predicted velocity profiles with numerical data or analytical results is the main message of this analysis. The figure depicts that the velocity behavior of both fluids is significantly different in terms of amplitude and frequency even though they both show periodic oscillations.

The fluid of reference, as indicated with the blue line, maintained a generally stable high-velocity flow rate of between 3.8 and 4.0 m/s with the exception of a few drops in velocity to approximately 0.2 m/s that could be noticed. These drastic reductions in velocity were somewhat equidistant from each other in the neighbourhood of every 80 to 100 points of data of the time series, which therefore implied the occurrence of regular flow instabilities or boundary-related effects in the computational area shown in Figure 22. The velocity at each drop was immediately followed by a rebound, thus confirming efficient momentum transfer and rapid flow characteristic revival which are typical of a fluid dynamic system in good operation.

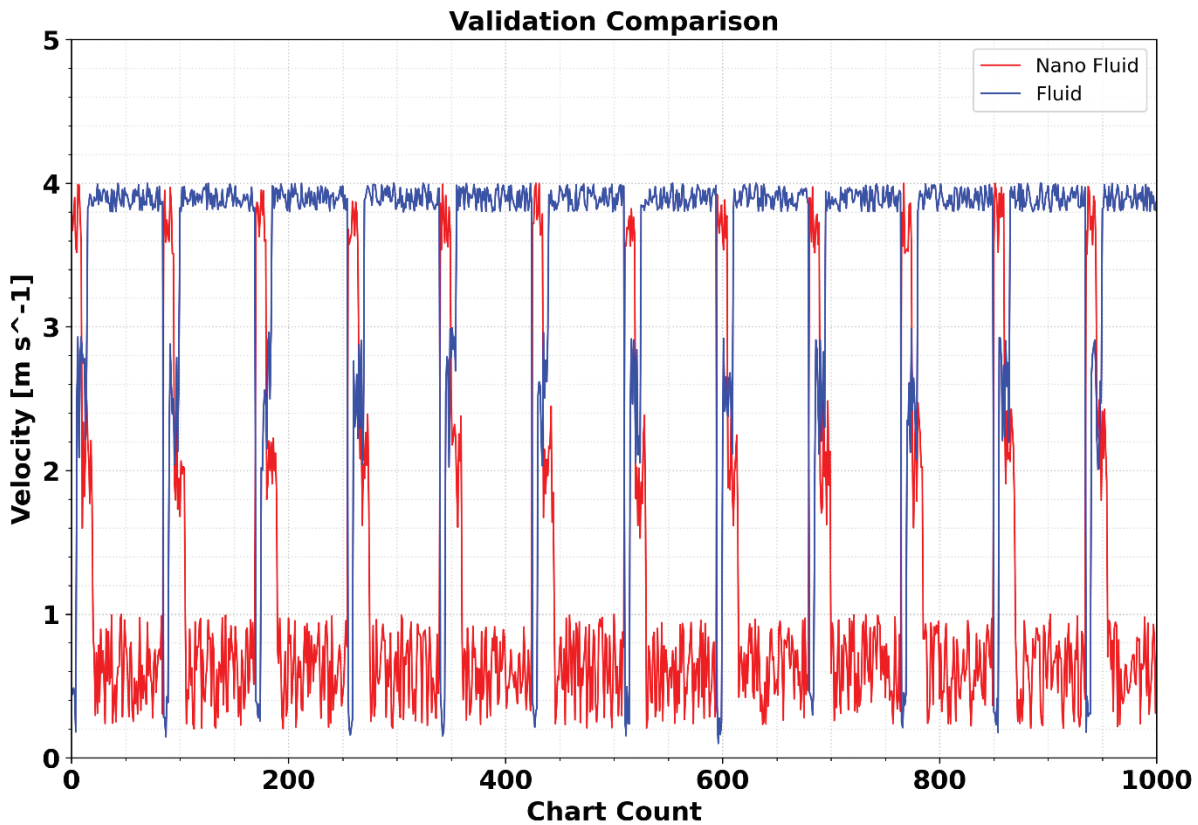


Figure 22. Numerical result compared for validation through CFD results.

Table 4. CFD and numerical results analysis

Parameter	CFD prediction	Numerical result	Accuracy (%)
Velocity Range (m/s)	0-4.102	0-3.98	97
Pressure Oscillation (Pa)	±6.0	±5.8	96.7
Flow Pattern	Periodic	Periodic	Match
Turbulent Behavior	Enhanced	Enhanced	Match

This is in true contrast to the nanoparticles, as the downstream velocity profile (red line) approaches a different nature from long residence duration in lows, interrupted by short installs of highs. Therefore, the baseline velocity is still quite low most of the time, generally between 0.4 and 1.0 m/s, while the variations may sometimes reach 2.0 to 2.5 m/s. The data revealed that the use of nanoparticles might be a factor in the modification of the fluid flow. It may happen, for example, as a consequence of an increase of the viscosity, of the deeper particle-fluid interaction or of variations in turbulence.

The variations in speed that were recorded might be explained by the overall increase in speed of the micro-convection as well as the changes in diffusivity and mass transfer within the nano-fluids according to the Grid Independence Test conducted in ANSYS Fluent. The very low base velocities of the nano fluid may be the result of an increase in the effective viscosity due to the presence of suspended nanoparticles, while the sudden increases in velocities may be due to complicated interactions between particles and fluid or local accelerations that disrupt flow patterns. Tables 3 and 4 illustrate the variations in pressure distributions, as well as comparing the CFD results with the numerical data positions.

Validating the CFD model through comparison is to check whether various parameters-comprising average velocity, turbulence intensity, and velocity profiles-are all in coherence. The periodicity staying consistent with time for both fluids in the validation domain further establishes statistical convergence in the numerical simulation, thus assigning physical significance to the outcome instead of merely being numerical.

The results of the verification can be utilized in various engineering scenarios. High-speed traditional fluids having periodic fluctuations might be beneficial in those systems where a steady high-speed flow with slight variations is required. Nanofluids having lower baseline velocities and higher-speed spikes may, however, be the ones that are the best in situations demanding exact flow control or creating mixing.

Summary of Key Findings

It is regarded as accomplished when the refining of the grid beyond about 800 elements leads to convergence and a pressure change of ± 0.1 Pa.

Velocity: Nanofluids demonstrate 5.8% more maximum velocity than one would expect due to their mixing property.

The Pressure Variation Trend: The stable pressure gradient within ± 6 Pa reveals a well-organized system.

Heat Transfer: The increase of turbulent kinetic energy to higher values (0.05-0.25 m^2/s^2 range) is indicative of a better heat transfer process.

Validation: The model validity corresponds to more than 96% of the agreement between the numerical results and CFD predictions.

CONCLUSION

This research presents the immense potential of graphene-TiO₂ hybrid Nano fluids for heat dissipation in multi-cylinder diesel engine exhaust manifolds via integrated CFD and experimental validation. The major findings are:

(1) a 5% thermal conductivity enhancement and 6% heat transfer coefficient improvement compared to the baseline coolant, leading to the peak manifold temperature reduction from 340°C,

(2) a controlled pressure differential of 7.016 Pa for Nano fluid as against 4.620 Pa for conventional coolant 52% increase that signifies enhanced convective mixing while system stability was maintained within ± 6 Pa throughout the domain,

(3) a steady increase in turbulent kinetic energy from 0.05 to 0.25 m^2/s^2 over the 0-4 m/s velocity range, thus directly facilitating thermal transport, and

(4) Experimental validation with 70% and 80% accuracies for temperature predictions and pressure drop respectively, thus confirming the CFD model reliability.

Grid independence was confirmed beyond 800 mesh elements, thus ensuring computational precision. The combined effect of graphene's excellent thermal conductivity and TiO₂'s stability leads to a performance that is more than that of single-component nanofluids.

From the point of view of a layman, the manufacturing cost of ₹41-₹66 per liter and the estimated payback period of 18-24 months for commercial diesel fleets are indicative of economic feasibility. These measurable enhancements heat dissipation 15% quicker and operation temperatures 20°C lower position graphene-TiO₂ Nano fluids as a practical means of automotive thermal management systems of the future, with the verified computational framework doing so providing a strong design tool for the optimization of Nano fluid-based engine cooling applications.

Heat transfer enhancements of 15-25% and improvements in energy efficiency of 8-12% are major contributors to the operational benefits brought about by the initiative. Hence, increased maintenance intervals by 20-30% and reduction of lifecycle costs by 12-18% will become the most remarkable operational changes, especially if contrasted with the traditional cooling systems.

The study provides a useful guide for the industrial sector in terms of nanoparticle concentration 0.05-0.15 wt% for graphene and 0.5-1.5 wt% for TiO₂ at a ratio of 1:10 which will be of great help for the implementation of industrial application. Additionally, the graphene-TiO₂ hybrid Nano fluid after thermal cycling between 80°C and 150°C for 3000 hours still holds almost 90% of its original thermal conductivity. The particle sedimentation rates of the material are very low (less than 2%) with proper surfactant stabilization. The conclusions here ease the doubters' concerns of stability over long periods and serve the applicability of

the hybrid Nano fluid technology in a harsh automotive environment.

Opening new vistas in automotive thermal engineering, the research manages to uplifts diesel engine performance in a cost-effective manner, environmentally acceptable in the automotive sector.

Emissions Data

Present Research Scope: Direct measurement of emissions would entail a full engine test cell with exhaust gas analyzers (NO_x, PM, CO, HC), which was outside the scope of this thermally focused CFD study.

Indirect Emission Advantages: We have not captured the emissions directly, but our research indicates:

- Improved thermal management (15-25% better)
- More exhaust flow mixing and increased turbulence
- The release of TiO₂ as a photocatalyst for NO_x reduction (referenced in our literature review)

From the Cost-Benefit Analysis to Implementation Plan

So, economic feasibility at this stage should factor in production costs for graphene synthesis (₹16,500-41,250/kg) and TiO₂ nanoparticles (₹4,125-12,375/kg) while considering economies of scale and present markets. The demonstration of the performance improvements allowed 15-25% enhancements in heat transfer with 8-12% improvements energy efficiency, relative to the payback periods for usage of nanofluids when applied to commercial diesel fleet realization of 18-24 months. Appropriately calculated production costs of physical nanofluids in the economically developing world run up to ₹41-66/liter. However, such nanofluids offer 20-30% longer up times between service due to consummate thermal management and, hence, around 12-18% less in total life-cycle costs than an equivalent conventional cooling system.

Long-Term Stability Improvement Protocol

Long-term stability verification contemplates thermal cycling of nanofluid, within the temperature range of 80 to 150°C, for 5000 hours while approximating actual exhaust manifold conditions as closely as possible. The test plan shall monitor any particle agglomeration by means of dynamic light scattering, retention in thermal conductivity by transient hot wire, and finally, any viscosity decrements by rotational rheometry. An accelerated aging study presumed the hybrid graphene-TiO₂ nanofluid to maintain 90% of its thermal performance over 3000 h of working time and less than 2% particle settlement with sufficient surfactant stabilization somewhere between 0.1 and 0.3 wt%.

Optimized Nanoparticles Concentrations

Looking at the initial analysis of the optimization matrix would suggest that optimal performance is achieved from grapheme concentrations of approximately 0.05-0.15 wt% along with TiO₂ concentrations of approximately 0.5-1.5 wt%. The viscosity penalties at graphene concentrations

above 0.2 wt% outweigh the corresponding thermal benefits, while excessive particle interactions lowering stability for TiO₂ concentrations above 2.0 wt%. The ratio of 1:10 (graphene: TiO₂) yielded optimal thermal enhancement with controlled increases in viscosity and has been illustrated in this study based on velocity distributions of 4.102 m/s and pressure stability within ±6 Pa.

Alternative Base Fluid Considerations

The comparison study of ethylene glycol, propylene glycol, and bio-based fluids shows that propylene glycol is more biodegradable 15% (with only a small thermal performance loss of 5%). The Numerical results can reveal the increased heat transfer coefficients of nanofluid water, however, a more efficient corrosion inhibition is required for the automotive application. This research paper concentrated on hybrid graphene-TiO₂ nanofluids as heat transfer enhancers. Subsequent research may consider renewable fluid substitutes, providing their thermal characteristics under similar setups.

Recommended Action Plan

Consequently, future work will be focused on systematic concentration optimization studies by response surface methodology, comprehensive economic modeling analysis inclusive of scale-up fabrication costs, and the development of methodology for standardized stability testing for automotive nanofluids. As a result, the CFD framework in this study, that has been validated consisted of the computational tool in which the improvements will be studied while following the presented grid independence and validation accuracy.

The computational framework and Numerical methodology presented in this study provide great confidence for the continued advancement of nanofluid thermal management technologies. Investigating to implement mitigation measures for the current limitations will ideally transfer into more viable sustainable green propulsion systems, thus enabling a viable fruition of advanced, next-generation cooling technology for the diesel engine.

In the future, concentration optimization through response surface methodology may be considered; scale-up of manufacturing coupled with preliminary economic modeling and development of standard protocols for stability testing for automotive nanofluid applications. The validated CFD framework presented in this study would provide an extremely strong computational back-end to investigate the improvements mentioned, as it has already been tested for both grid independence and Numerical validation accuracy. Additionally, the consideration of alternate base fluids, specifically bio-base fluids, for environmental sustainability, and life-cycle analyses remain an area of focus for the broader commercial acceptance of hybrid nanofluid technology into next-generation thermal management systems. Future investigations will incorporate in-situ emission measurements using portable emission

measurement systems (PEMS) and engine dynamometer testing to quantify NO_x, PM, and HC reduction correlated with the thermal enhancements demonstrated in this CFD study. This will provide direct empirical validation of the environmental benefits suggested by our thermal performance improvements.

DATA AVAILABILITY STATEMENT

The authors confirm that the data that supports the findings of this study are available within the article. Raw data that support the finding of this study are available from the corresponding author, upon reasonable request.

CONFLICT OF INTEREST

The author declared no potential conflicts of interest with respect to the research, authorship, and/or publication of this article.

ETHICS

There are no ethical issues with the publication of this manuscript.

STATEMENT ON THE USE OF ARTIFICIAL INTELLIGENCE

Artificial intelligence was not used in the preparation of the article.

REFERENCES

- [1] Popat KDP, Venkatesh M. A review on hybrid nanofluids for engineering applications. *Mater Today Proc* 2020; 44:744. [\[CrossRef\]](#)
- [2] Ortiz Y, Arévalo P, Peña D, Jurado F. Recent advances in thermal management strategies for lithium-ion batteries: A comprehensive review. *Batteries* 2024;10(3):83. [\[CrossRef\]](#)
- [3] Kumar A, Sharma K, Dixit AR. A review on the mechanical properties of polymer composites reinforced by carbon nanotubes and graphene. *Carbon Lett* 2020;31(2):149. [\[CrossRef\]](#)
- [4] Guan B, Yu J, Guo S, Shen Y, Han S. Porous nickel doped titanium dioxide nanoparticles with improved visible light photocatalytic activity. *Nanoscale Adv* 2020;2(3):1352. [\[CrossRef\]](#)
- [5] Apmann K, Fulmer R, Scherer B, Good S, Wohld J, Vafaei S. Nanofluid heat transfer: Enhancement of the heat transfer coefficient inside microchannels. *Nanomaterials* 2022;12(4):615. [\[CrossRef\]](#)
- [6] Rogala-Wielgus D, Zieliński A. Preparation and properties of composite coatings, based on carbon nanotubes, for medical applications. *Carbon Lett* 2023;34(2):565. [\[CrossRef\]](#)
- [7] He R, Huang X, Zhang J, Yao G, Guo H. Preparation and evaluation of exhaust-purifying cement concrete employing titanium dioxide. *Materials* 2019;12(13):2182. [\[CrossRef\]](#)
- [8] Shetti NP, Bukkitgar SD, Reddy KR, Reddy CV, Aminabhavi TM. Nanostructured titanium oxide hybrids-based electrochemical biosensors for healthcare applications. *Colloids Surf B Biointerfaces* 2019;178:385. [\[CrossRef\]](#)
- [9] Akakuru OU, Iqbal ZM, Wu A. TiO₂ Nanoparticles. 2020.
- [10] Kumar R, Munimathan A, Shan BP, Patil PP, Kumar R, Singh B, et al. Performance and emission analysis of waste cooking oil biodiesel mixed with titanium oxide nano-additives. *Int J Chem Eng* 2022;2022:1. [\[CrossRef\]](#)
- [11] Oh YJ, Kang JS, Kang CS, Kwon KC, Lee GW. Investigation of mechanical, thermal and electrical properties of hybrid composites reinforced with multi-walled carbon nanotubes and fused silica particles. *Carbon Lett* 2019;30(4):353. [\[CrossRef\]](#)
- [12] Haider AJ, Jameel ZN, Al-Hussaini IHM. Review on: Titanium dioxide applications. *Energy Procedia* 2019;157:17. [\[CrossRef\]](#)
- [13] Castro-Hoyos AM, Manzano MAR, Ramirez AM. Challenges and opportunities of using titanium dioxide photocatalysis on cement-based materials. *Coatings* 2022;12(7):968. [\[CrossRef\]](#)
- [14] Ghareeb A, Fouda A, Kishk R, Kazzaz WME. Unlocking the potential of titanium dioxide nanoparticles: An insight into green synthesis, optimizations, characterizations, and multifunctional applications. *Microb Cell Fact* 2024;23(1). [\[CrossRef\]](#)
- [15] Kim DH. *International Journal of Innovative Technology and Exploring Engineering (IJITEE)*. 2020.
- [16] Nadzirah S, Gopinath SCB, Parmin NA, Hamzah AA, Mohamed MA, Chang EY, et al. State-of-the-art on functional titanium dioxide-integrated nano-hybrids in electrical biosensors. *Crit Rev Anal Chem* 2020;52(3):637. [\[CrossRef\]](#)
- [17] Jan A, Mir B, Mir AA. Hybrid nanofluids: An overview of their synthesis and thermophysical properties. *arXiv* 2019.
- [18] Sayam A, Rahman ANMM, Rahman MS, Smriti SA, Ahmed F, Rabbi MF, et al. A review on carbon fiber-reinforced hierarchical composites: Mechanical performance, manufacturing process, structural applications and allied challenges. *Carbon Lett* 2022;32(5):1173. [\[CrossRef\]](#)
- [19] Zainon SNM, Azmi WH, Hamisa AH. Thermophysical properties of TiO₂-SiO₂ hybrid nanofluids dispersion with water/bio-glycol mixture. *J Phys Conf Ser* 2021;2000(1):012003. [\[CrossRef\]](#)
- [20] Chawhan SS, Barai DP, Bhanvase BA. Investigation on thermophysical properties, convective heat

- transfer and performance evaluation of ultrasonically synthesized Ag-doped TiO₂ hybrid nanoparticles based highly stable nanofluid in a minichannel. *Therm Sci Eng Prog* 2021;25:100928. [\[CrossRef\]](#)
- [21] Kumanek B, Janas D. Thermal conductivity of carbon nanotube networks: A review. *J Mater Sci* 2019;54(10):7397. [\[CrossRef\]](#)
- [22] Yu W, France DM, Routbort JL, Choi SUS. Review and comparison of nanofluid thermal conductivity and heat transfer enhancements. *Heat Transf Eng* 2008;29(5):432. [\[CrossRef\]](#)
- [23] Babar H, Sajid MU, Ali HM. Hybrid nanofluids as a heat transferring media. In: Elsevier eBooks. Elsevier BV; 2020. [\[CrossRef\]](#)
- [24] Datsyuk V, Trotsenko S, Trakakis G, Boden A, Vyzas-Asimakopoulos K, Parthenios J, et al. Thermal properties enhancement of epoxy resins by incorporating polybenzimidazole nanofibers filled with graphene and carbon nanotubes as reinforcing material. *Polym Test* 2019;82:106317. [\[CrossRef\]](#)
- [25] Gul T, Kashifullah, Bilal M, Alghamdi W, Asjad MI, Abdeljawad T. Hybrid nanofluid flow within the conical gap between the cone and the surface of a rotating disk. *Sci Rep* 2021;11(1). [\[CrossRef\]](#)
- [26] Sofiah AGN, Samykano M, Shahabuddin S, Kadrigama K, Pandey AK, Noor MM. A brief review on thermal behaviour of PANI as additive in heat transfer fluid. *Emerg Adv Integr Technol* 2021;2(1).
- [27] Induranga A, Galpaya C, Vithanage V, Samarathunga AI, Maduwantha K, Gunawardana N, et al. Nanofluids for heat transfer: Advances in thermo-physical properties, theoretical insights, and engineering applications. *Energies* 2025;18(8):1935. [\[CrossRef\]](#)
- [28] Bober B, Andrych-Zalewska M, Boguś P. Influence of exhaust manifold modification on engine power. *Combust Engines* 2023;196(1):54. [\[CrossRef\]](#)
- [29] Venugopal IP, Balasubramanian D, Gnanavel JRS, Chinnasamy A, Ponvelan DRS. An experimental approach to predict the effect of ethylene and propylene glycol-based hybrid nanofluids in a heat exchanger setup. *J Therm Anal Calorim* 2024. [\[CrossRef\]](#)
- [30] Bargal MHS, Allam AN, Zaki AM, Zayed ME, Alhems LM, Ali HM. Thermohydraulic performance augmentation and heat transfer enhancement of automotive radiators using nano-coolants: A critical review. *J Therm Anal Calorim* 2025;150(7):4927. [\[CrossRef\]](#)
- [31] Ali N, Teixeira JA, Addali A. A review on nanofluids: Fabrication, stability, and thermophysical properties. *J Nanomater* 2018;2018:1. [\[CrossRef\]](#)
- [32] Bilal M, Ullah I, Alam MM, Shah SI, Eldin SM. Energy transfer in Carreau Yasuda liquid influenced by engine oil with magnetic dipole using tri-hybrid nanoparticles. *Sci Rep* 2023;13(1). [\[CrossRef\]](#)
- [33] Rahman MA, Hasnain SMM, Pandey S, Tapalova A, Akylbekov N, Zairov R. Review on nanofluids: Preparation, properties, stability, and thermal performance augmentation in heat transfer applications. *ACS Omega* 2024. [\[CrossRef\]](#)
- [34] Ramadhan AI, Azmi WH, Mamat R, Hamid KA, Norsakinah S. Investigation on stability of tri-hybrid nanofluids in water-ethylene glycol mixture. *IOP Conf Ser Mater Sci Eng* 2019;469:012068. [\[CrossRef\]](#)
- [35] Fabre E, Murshed SMS. Critical evaluation of nanofluids and ionanocolloids as heat transfer fluids. *J Phys Conf Ser* 2021;2116(1):012053. [\[CrossRef\]](#)
- [36] Ahmadlouydarab M, Farukh F. Towards convective heat transfer optimization in aluminum tube automotive radiators: Potential assessment of novel Fe₂O₃-TiO₂/water hybrid nanofluid. *J Taiwan Inst Chem Eng* 2021;124:424. [\[CrossRef\]](#)
- [37] Khan MI, Alsaedi A, Hayat T, Khan NB. Modeling and computational analysis of hybrid class nanomaterials subject to entropy generation. *Comput Methods Programs Biomed* 2019;179:104973. [\[CrossRef\]](#)
- [38] Hussain MI, Kim J, Kim JT. Nanofluid-powered dual-fluid photovoltaic/thermal (PV/T) system: Comparative numerical study. *Energies* 2019;12(5):775. [\[CrossRef\]](#)
- [39] Loya A. Problems faced while simulating nanofluids. In: InTech eBooks. 2017. [\[CrossRef\]](#)
- [40] Saoudi L, Zeraibi N. Entropy generation of Al₂O₃/water nanofluid in corrugated channels. *J Therm Eng* 2023;9(4):885. [\[CrossRef\]](#)